









Consistency of Mechanical Properties of 3D Printed Strain Hardening Cementitious Composites Within One Printing System

Karsten Nefs¹ (✉) , A. L. van Overmeir² , Theo A. M. Salet¹, A. S. J. Suiker¹ ,
B. Šavija² , E. Schlangen² , and Freek Bos¹ 

¹ Eindhoven University of Technology, Eindhoven 5600 MB, The Netherlands
k.nefs@tue.nl

² Delft University of Technology, Delft 2628 CN, The Netherlands

Abstract. Previous research has shown that the material properties of a three-dimensional printed strain hardening cementitious composite (3DP-SHCC) can significantly vary, depending on the printing system with which it is produced. However, limited research has been performed on the reproducibility of hardened mechanical properties under *identical* printing conditions. In this study, the consistency of hardened properties, including compressive strength, flexural strength and deflection, and tensile strength and strain, was tested from materials printed during three separate but identical printing sessions. The research shows that with 3DP-SHCC, significant variations in mechanical properties between printing sessions can be expected.

Keywords: SHCC · 3DCP · Printing control · Variation

1 Introduction

The limited ductility of 3D printable mortars is still one of the bigger challenges within the field of 3DCP. Nevertheless, a strain hardening cementitious composite (SHCC) is a material that displays a relatively ductile behaviour, and has been successfully applied in 3D concrete printing [1]. The effect of different printing systems on the mechanical properties of 3DP-SHCC was investigated by Figueiredo et al. [2]. Here it was found that both the mechanical and the physical properties of 3DP-SHCC specimens manufactured at Delft University of Technology (TUD) and Eindhoven University of Technology (TU/e) were significantly different, which was mainly attributed to the differences in equipment (geometries, brands, types, specifications).

However, the consistency of mechanical properties of 3DP-SHCC elements printed on the same printing system, but over different printing sessions, was not investigated and is therefore the topic of the current study.

2 Methodology

2.1 Materials

The material composition of the 3DP-SHCC mix used in the 3D printing experiments is presented in Table 1. A detailed description of the deployed mixing procedure can be found in Van Overmeir et al. [3]. The material is mixed in batches with a Hobart A200N mixers. Due to the maximum torque capacity of the mixer, the batches were limited to a volume of 3.5 L.

Table 1. 3DP-SHCC composition, in [kg/m^3] including viscosity modifying agent (VMA), super plasticizer (SP) and polyvinyl alcohol fibres (PVA).

Blast furnace slag	Cement 42.5 N	Silica fume	Limestone	Sand ($<250 \mu\text{m}$)	Water	VMA	SP	PVA
262.8	470.4	32.9	583.9	317.5	400.2	3.06	2.68	26.0

2.2 Printing Sessions

Three identical printing sessions were performed in 2021, on the 26th of October, and the 2nd and 4th of November, which are referred to as printing sessions “A”, “B” and “C”, respectively. The ambient conditions for each of these printing sessions were similar: 21.4 °C with a relative humidity (RH) of 44.5%, 21.7 °C with an RH of 37.0%, and 21.4 °C with an RH of 35.5%, respectively. These printing sessions were followed by an experimental program to assess the consistency of the mechanical properties in the hardened state. Each printing session resulted in 10 beams with a length of 800 mm and a height of 6 layers. Printing was done with a downflow nozzle ($40 \times 12 \text{ mm}^2$) at a speed of 28.5 mm/s. Due to small deformations after deposition of the material, an effective layer cross-section of approximate $40 \times 11 \text{ mm}^2$ was achieved, resulting in an effective cross-section of the beam of $66 \times 40 \text{ mm}^2$. The printed objects were covered with plastic. Wet cloths were placed inside to keep the relative humidity close to 100%. After 1 day of curing, the beams were submerged in water. On the 7th day the beams were sawn into the specific specimens required for each test. Afterwards, the specimens were placed back into the water, and were taken out again one day before testing.

2.3 Compression Test and Apparent Density

Compression tests were performed on cuboidal specimens 28 days after the printing session took place. The specimens were sawn to a size of $35 \times 35 \times 35 \text{ mm}^3$ ($\pm 1 \text{ mm}$). The tests were performed on a Automax 5 test rig according to NEN-EN 196-1, applying a compression rate of 2400 N/s. The compressive strength was determined in the length-, width- and height-directions of the printed beam, indicated with I, II, and III (3 \times 6 samples) as defined by Wolfs [7]. For each of the cubes, the weight and dimensions were measured directly before the tests were performed, after drying for 1 day.

2.4 4-point Bending Test

In order to assess the flexural strength and deflection capacity of SHCC, a 4-point bending test was performed, in accordance with the procedure described in [4]. For this test, 5 specimens for each printing session were sawn into slabs with dimensions of $150 \times 30 \times 10 \text{ mm}^3$. The effective span of the slabs corresponded to the distance between the supports, and was equal to 120 mm. The load was applied with two steel rods spaced 40 mm. The deflection rate imposed on the Instron 8872 test apparatus was equal to 0.005 mm/s. The test was performed 29 days after the printing session took place.

2.5 Uni-axial Tensile Test

The uniaxial tensile strength and deformation capacity were determined by performing an uniaxial tensile test. The background of the test procedure is presented in [5], which was slightly modified to avoid failure of the adhesive bond between the specimen and the test set-up. For this purpose, steel plates were attached at two sides of the specimens to increase the adhesive area. From each printing session, 6 specimens with a size of $250 \times 40 \times 20 \text{ mm}^3$ were prepared, and subsequently tested 27–28 days after printing. The test was performed on an Instron 5985 test apparatus in a deformation-controlled fashion, applying a deformation rate of $5 \mu\text{m/s}$.

2.6 Statistical Methods

Due to the limited number of samples available for the compression test (18), 4-point bending test (5) and uni-axial tensile test (6), the statistical distribution of the test results is not immediately obvious. Therefore, the Shapiro-Wilk [6] test method was used to assess whether the results from a single session were normally distributed.

If so, the Student's t-test was subsequently applied to evaluate whether the results from individual sessions could originate from the same normal distribution. In this way, the statistical significance of the difference in results from samples prepared from different printing sessions could be established.

3 Results and Discussion

3.1 Compressive Strength and Apparent Density

The average compressive strength and apparent density for the specimens from printing sessions A, B and C are shown in Fig. 1 for each of the three directions. The compressive strength obtained from printing session A is, respectively, 11.69% and 10.59% higher than that from printing sessions B and C. For printing sessions A and C, the average compressive strength is maximal in direction II while for printing session B direction I gives the maximal average compressive strength. Note further that for session B, the standard deviation of the compressive strength is the largest in all three directions. The apparent density for printing session B also is the lowest and has the largest standard deviation.

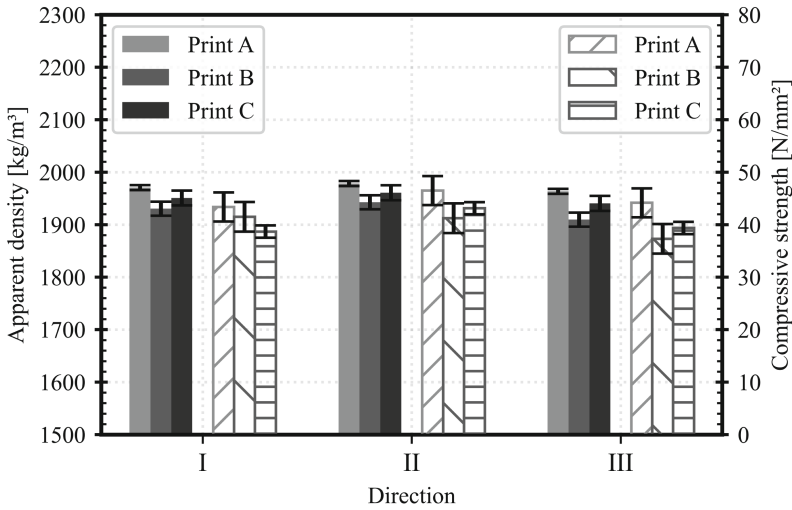


Fig. 1. Compressive strength (after 28 days of curing) and apparent density for specimens from printing session A, B and C, in directions I–III, as defined by Wolfs [7].

3.2 4-point Bending Test

Figure 2a shows a representative bending stress-deflection curve obtained from a 4-point bending test on specimens constructed from each of the three printing sessions. The average maximum bending stress and average maximum deflection are shown in Table 2. It can be observed that the specimen from printing session B shows a lower average maximum bending stress at a significantly lower deflection capacity compared to the specimens from printing sessions A and C.

Table 2. Average maximum bending stress and deflection (29 days), and average maximum uniaxial stress and strain (27–28 days).

Printing session	Average maximum bending stress [N/mm ²] (±STD)	Average deflection at max bending stress [mm] (±STD)	Average maximum uniaxial stress [N/mm ²] (±STD)	Average strain at max uniaxial stress [%] (±STD)
Print A	8.49 ± 1.13	5.12 ± 1.10	2.92 ± 0.17	0.86 ± 0.43
Print B	6.03 ± 1.01	2.63 ± 1.26	2.24 ± 0.38	0.41 ± 0.52
Print C	7.61 ± 1.10	4.09 ± 0.50	2.86 ± 0.13	1.15 ± 0.73

3.3 Uniaxial Tensile Test

Figure 2b illustrates a representative stress-strain curve measured in the uniaxial tensile test on a specimen from each of the three printing sessions. The average maximum uniaxial stress and average maximum strain at the maximal stress are listed in Table 2. Similar as in the 4-point bending test, the uniaxial tensile tests show a lower strength for the specimen from session B, and further a considerably lower deformation (i.e. strain). Actually, in both types of tests the measured deformation capacity seems to be more sensitive to the printing session, than the measured strength.

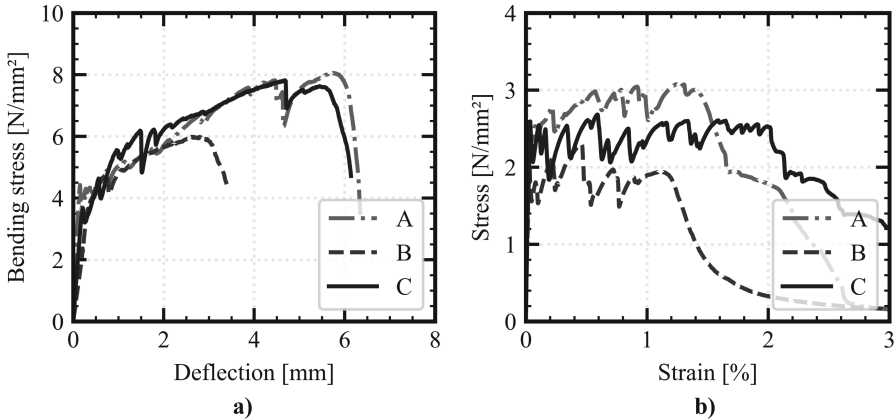


Fig. 2. Representative bending stress-deflection curves of 4-point bending test (a) and stress-strain curves of the uniaxial tensile test (b) for printing sessions A, and B and C.

3.4 Statistical Analysis

The Shapiro-Wilk [6] test method was applied to the test data and shows that the measured compressive strength, bending strength and tensile strength from specimens of each of the three printing sessions can be considered as normally (Gaussian) distributed. The statistical values found for the compressive strength are: $W = 0.979, p = 0.94$; $W = 0.971, p = 0.82$; $W = 0.956, p = 0.52$; for the bending strength they are: $W = 0.983, p = 0.95$; $W = 0.909, p = 0.46$; $W = 0.968, p = 0.87$; and for tensile strength they are: $W = 0.877, p = 0.25$; $W = 0.921, p = 0.51$; $W = 0.943, p = 0.68$; for printing sessions A, B, and C respectively. Based on these findings Student's t-tests were subsequently performed. Table 3 indicates which results are likely to originate from the same distribution and which not. These results are consistent for both tensile tests (bending and uniaxial), indicating an agreement in distributions for sessions A and C. However, a different finding for the compressive test is obtained, as this test shows an agreement between session B and C, but not between A and C.

Table 3. Comparison of the distribution of results from different printing sessions with the use of the Student's t-test (green/✓; probably from the same distribution (p value > 0.05), (red/✗; probably not from the same distribution (p value < 0.05)).

Printing session	T-test (Compressive strength)			T-test (Bending stress)			T-test (Uniaxial stress)		
	Print A	Print B	Print C	Print A	Print B	Print C	Print A	Print B	Print C
	Print A	-	✗	✗	-	✗	✓	-	✗
Print B	✗	-	✓	✗	-	✗	✗	-	✗
Print C	✗	✓	-	✓	✗	-	✓	✗	-

4 Conclusions

This aim of this study is to evaluate the consistency of mechanical properties of 3DP-SHCC, obtained from separate but identical printing sessions. It may be concluded that:

- Objects printed in separate printing sessions can display significant (but not dramatic) differences in their mechanical properties.
- Properties related to deformation capacity (i.e., deformation in bending and strain in uniaxial tension) are quantitatively more strongly affected by the printing session than tensile strength properties (i.e., bending- and uniaxial strength).
- The consistency between different printing sessions (i.e., whether results may have originated from the same statistical distribution) is not necessarily the same for compressive and (bending and uniaxial) tensile strength properties.

From the above research results, it is concluded that several separate printing sessions are required to make unambiguous quantitative statements about mechanical properties of 3DP-SHCC (e.g. in the context of standardized strengths). Further research is necessary to determine whether this also applies to other types of printable mortars.

Acknowledgements. This research was funded through the NWO Open Technology Program, project ‘High Performance 3D Concrete Printing’, grant number 17251.

References

1. Figueiredo, S.C., et al.: An approach to develop printable strain hardening cementitious composites. *Mater. Des.* **169**, 107651 (2019). <https://doi.org/10.1016/j.matdes.2019.107651>
2. Figueiredo, S.C., et al.: Quality assessment of printable strain hardening cementitious composites manufactured in two different printing facilities. In: Bos, F.P., Lucas, S.S., Wolfs, R.J.M., Salet, T.A.M. (eds.) DC 2020. RB, vol. 28, pp. 824–838. Springer, Cham (2020). https://doi.org/10.1007/978-3-030-49916-7_81
3. Linde, A., van Overmeir, S.C., Figueiredo, B.Š, Bos, F.P., Schlangen, E.: Design and analyses of printable strain hardening cementitious composites with optimized particle size distribution. *Constr. Build. Mater.* **324**, 126411 (2022). <https://doi.org/10.1016/j.conbuildmat.2022.126411>

4. Figueiredo, S.C., et al.: Mechanical behavior of printed strain hardening cementitious composites. *Materials* **13**(10), 1–2 (2020). <https://doi.org/10.3390/ma13102253>
5. Ogura, H., et al.: Developing and testing of strain-hardening cement-based composites (SHCC) in the context of 3D-printing. *Materials* **11**(8), 1–18 (2018)
6. Shapiro, S.S., Wilk, M.B.: An analysis of variance test for normality (complete samples). *Biometrika* **52**(3/4), 591 (1965). <https://doi.org/10.2307/2333709>
7. Wolfs, R.: Experimental characterization and numerical modelling of 3D printed concrete: controlling structural behaviour in the fresh and hardened state. Ph.D. thesis, Eindhoven University of Technology (2019)